*Applied Science and Engineering Progress, Vol. 20, No. 4, 2027, 8376*

Research Article

# Valorization of Jackfruit Seed Waste for Composite Film Preparation: Property Enhancement via Bacterial Cellulose Reinforcement

Arnon Khamkeaw*, Thanyaruk Chatthong, Tayida Phosang, and Vanarat Phakeenuya
Department of Biotechnology, Faculty of Applied Science, King Mongkut's University of Technology North Bangkok, Bangkok, 10800, Thailand

Suttinun Phongtamrug
Department of Industrial Chemistry, Faculty of Applied Science, King Mongkut's University of Technology North Bangkok, Bangkok, 10800, Thailand

* Corresponding author. E-mail: arnon.k@sci.kmutnb.ac.th DOI: 10.14416/j.asep.2026.11.002
Received: 14 July 2026; Revised: 1 October 2026; Accepted: 7 October 2026; Published online: 2 November 2026
© 2026 King Mongkut's University of Technology North Bangkok. All Rights Reserved

**Abstract**
Conventional plastic has become an essential element in the manufacturing of nearly all consumer products. However, it has emerged as a major contributor to environmental pollution and is difficult to biodegrade. This research therefore synthesizes composite films from jackfruit seed (JSF) reinforced with bacterial cellulose (BC) for a sustainable alternative. The structural, physical, chemical, and mechanical properties of Jackfruit Seed Starch-based composite films (JSF/BC) were investigated. The incorporation of BC fiber into the JSF composite film matrix significantly enhanced the water resistance, UV blocking, and thermal stability. By loading BC at 40 wt.%, the mechanical properties, such as tensile strength and elongation, were 0.74 MPa and 10.21%, respectively. JSF/BC composite films had a thermal stability at temperatures up to approximately 270 °C. JSF/BC composite films also exhibited a biodegradability of 72.1 - 100% within 15 days. The experimental results indicate that the composite film offers a green, high-performing alternative to conventional plastics, suitable for packaging and other short-term plastic products.

**Keywords**: Bacterial cellulose, Biodegradation, Biomass, Biomaterial, Composite, Jackfruit seed

## 1 Introduction

The increased usage of plastics is the main contributor to environmental pollution concerns because it is produced from non-renewable resources and exhibits slow degradation [1]-[3], leading to the production and development of biodegradable plastics from renewable resources [4]-[6]. The bioplastic composite material is an interesting product because it has biodegradability, naturality, reduced reliance on fossil sources, and a low carbon footprint [7], [8]. Numerous studies have explored the production of novel composites from biomass resources [9]-[12]. The most suitable sources for composite production are waste-derived agricultural crops. It offers a renewable, sustainable, cost-effective and highly accessible alternative [8], [13]. To meet the growing demands for sustainable and multifunctional composite materials, recent engineering developments have explored diverse combinations of biopolymer matrices, natural fibers, and functional particulate fillers. Recent studies have demonstrated significant mechanical and physical property enhancements in matrix-reinforcement systems, such as natural fiber-reinforced polymer composites [14], polymer networks integrated with natural gums [15], discarded tube light particle-reinforced epoxy matrices [16], ultrafine bio-based fillers like coconut shell powder in epoxy networks [17], vinyl ester hybrid composites reinforced with smoked cigarette filter fibers, silane-treated palm fibers, and duck eggshell bio-fillers [18], as well as PLA-based hybrid biocomposites incorporating flax fibers and agricultural waste bio-fillers [19].

Among different types of waste-derived agricultural crops, jackfruit seed is one of the interesting biomasses for composite production due to its high starch content (about 30% of fresh seed

Applied Science and Engineering Progress, Vol. 20, No. 4, 2027, 8376

weight) [20]. In many Asian countries, especially Thailand, the jackfruit seed can be obtained in large quantities and at low cost or even free compared to alternatives such as corn or rice starch because it is normally discarded as waste from the food and agriculture industries. Nguyen *et al.,* [20] successfully synthesized a composite from jackfruit seed starch. Due to its environmental friendliness and high value-added potential, it is a strong candidate for future materials. However, the jackfruit seed-based composite film (JSF) has poor mechanical properties. Therefore, the mechanical properties necessitate the development of fillers and composites.

To improve the mechanical properties of composites, bacterial cellulose (BC) is a noticeable new material for reinforcing materials. BC is a major biopolymer and renewable material of high availability in Southeast Asia. BC is a cellulosic biomaterial that has come to the forefront as a promising renewable and sustainable material [21]-[23]. It is synthesized by bacteria, such as *Acetobacter xylinum* and *Komagataeibacter nataicola* [24], [25]. Compared to other bio-based fillers such as plant-derived cellulose nanocrystals (CNCs), lignin, and chitosan, BC exhibits distinct structural and functional superiorities [26]. While plant fibers require harsh acid hydrolysis or organosolv extraction to eliminate lignin and hemicellulose, resulting in environmental pollution and structural damage, BC is synthesized via microbial fermentation as a chemically pure cellulose hydrogel. The high density of accessible surface hydroxyl groups on the ultrafine BC nanofibrils facilitates robust interfacial hydrogen bonding with the amylose/amylopectin chains of JSF, establishing a highly effective reinforcement network superior to rigid isolated rod-like CNCs or particulate lignin fillers [26]. BC has a nanocellulose fiber matrix with distinctive properties, including its high degree of crystallinity, high tensile strength, high biocompatibility, and resistance to organic solvents [27]-[30]. BC is also recognized for its high purity, excellent mechanical properties, and ability to form 3D nanostructured networks [31]. In our previous work, we demonstrated the successful reinforcement of natural rubber with BC nanofibers [32]. These results indicated that BC is effective as a reinforcing additive. Based on these findings, incorporating BC nanofibers into a starch matrix could enable the development of the chemical, physical, and mechanical properties of the composite, such as water resistance, thermal stability, tensile strength, and biodegradability.

The scientific novelty of combining JSF and BC lies in exploiting their complementary molecular structures. The high density of surface hydroxyl groups on BC nanofibrils forms strong interfacial hydrogen bonds with the gelatinized JSF polymeric chains, creating a reinforced 3D interpenetrating network [33]. This synergistic interaction effectively compensates for the mechanical fragility and moisture vulnerability of JSF, offering a fully biodegradable, high-performance biocomposite derived entirely from agricultural byproducts and microbial synthesis.

Although starch-based and cellulosic films have been individually investigated, the primary novelty of this work lies in the formulation and comprehensive multi-scale characterization of green biocomposite films derived from JSF reinforced with BC nanofibrils. While jackfruit seed starch serves as an abundant, underutilized agro-industrial byproduct [34], its inherent brittleness and high moisture sensitivity severely restrict its application [35]. To overcome these limitations, this study provides the first systematic evaluation of how high-aspect-ratio BC nanofibrils systematically tailor the physical, quantitative crystallinity, multi-stage thermal degradation, and UV-blocking performance of JSF matrices. The findings demonstrate a sustainable, fully bio-based strategy to convert agricultural waste into high-performance, UV-shielding biocomposite films suitable for sustainable food packaging applications. In order to exploit food and agricultural wastes and improve composite properties, this research therefore produces composite films from jackfruit seed starch reinforced with BC in the range of 10 – 50 wt.% (wet basis). After the composite films were fabricated, the properties of the films were characterized to evaluate their suitability for future applications.

## 2 Materials and Methods

### 2.1 *Preparation of bacterial cellulose*

Bacterial cellulose (BC) was synthesized by *A. xylinum* strain AGR 60 using coconut water as the main medium. Then, 5.0% w/v sucrose, 0.05% w/v ammonium sulfate, and 1.0% v/v acetic acid were added as supplements. The 5% v/v *A. xylinum* AGR 60 was added to the medium and incubated at $30 \pm 2$ °C for 7 days. To eliminate the bacterial cells from the BC hydrogel structure, the BC hydrogel was immersed in 1% w/v sodium hydroxide for 24 h, and then it was treated with deionized (DI) water until pH was natural (Figure 1). Finally, BC was blended and

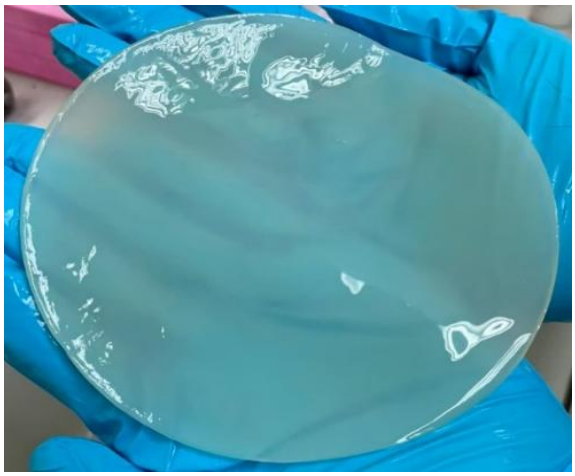


**Figure 1**: Image of BC.

homogenized thoroughly using a high-shear mixer at 5,000 rpm for 10 min at room temperature. The BC slurry had a measured solid content of 1.20 ± 0.15 wt.% (determined by drying a known wet mass at 110 °C until constant weight). The BC slurry was stored at 4 °C for future use.

### 2.2 *Extraction of jackfruit seed starch*

Jackfruit seeds, a food processing waste, were provided from a local Thai market. The seed outer skin was peeled off, then the peeled jackfruit seeds were washed with water to remove fruit flesh residue. After that, peeled jackfruit seeds were placed at65 °C for 48 h to remove the moisture, then the dried jackfruit seeds were mashed into a fine powder (100 mesh). The jackfruit seed powder was boiled in DI water at a temperature of 100 ºC for 40 min to extract starch. The slurry was centrifuged at 5,000 rpm for 30 min to separate the jackfruit seed residual, then the supernatant was deposited at 4 ºC for 24 h until the starch settled perfectly. Jackfruit seed starch sediment was separated using Whatman filter paper No. 1 to obtain wet starch. Next, the wet jackfruit seed starch was dried in a hot air oven (UF110, Memmert, Germany) at 65 °C for 48 h, and then the dried jackfruit seed starch was sieved with a strainer (AS 200, Retsch, USA) with a 100 mesh.

### 2.3 *Composite film preparation*

The 10 g of jackfruit seed starch was mixed with 5 mL of acetic acid, 10 mL of glycerol, and 100 mL of DI water, then the mixture was heated at 100 ºC for 30 min using a hotplate (C-MAG HS 7, IKA, Germany) under stirring at 200 rpm. After 20 min, BC was added in variations of 10, 20, 30, 40, and 50 wt.% (wet basis). in the mixture. After 25 min, the mixture was poured into a mold having 16 x 24 $cm^2$, set at room temperature for 3 h, and dried in a hot air oven at 35 ºC for 24 h. Then, the jackfruit seed film (JSF) was stored at room temperature for further use and named JSF/BC-x, where x was the percent of BC loading.

### 2.4 *Characterization*

The morphologies were observed by scanning electron microscopy (SEM) (QUANTA 450, FEI, USA). The film specimens were mounted onto aluminum stubs using conductive double-sided carbon tape and subsequently sputter-coated with a thin layer of gold under vacuum to provide electrical conductivity and prevent charge accumulation. The SEM micrographs were acquired at an accelerating voltage of 15 kV under high-vacuum conditions.

The surface functional groups were identified by Fourier transform infrared (FT-IR) (Spectrum 3TM, PerkinElmer, USA) spectroscopy equipped with an attenuated total reflectance (ATR) technique. Spectra were recorded in the wavenumber range of 4000 - 650 $cm^{-1}$ with a spectral resolution of 2 $cm^{-1}$ and an accumulation of 32 scans per sample at room temperature.

The mechanical properties were evaluated by a universal testing machine (UTM) (QC-506M1, Cometech, Taiwan). Prior to testing, all film specimens were cut into rectangular strips (15 mm × 100 mm). The film thickness was measured at five random positions along the specimen length using a digital micrometer (precision 0.001mm) to determine the average cross-sectional area. The UTM was operated with an initial grip distance (gauge length) of 100 mm and a crosshead speed of 5 mm/min at room temperature. All mechanical tests were performed in quintuplicate, and the average values with standard deviations were recorded.

The thermal stability and mass loss were demonstrated by thermogravimetric analysis (TGA) (TGA/DSC1, Mettler Toledo, Switzerland). The samples of approximately 7.3 ± 0.6 mg were placed in standard alumina pans. The analysis was conducted under a high-purity nitrogen atmosphere at a flow rate of 50 mL/min from 40 ºC to 900 ºC at a constant heating rate of 10 ºC/min. The onset decomposition temperature ($T_{onset}$), peak degradation temperature

Applied Science and Engineering Progress, Vol. 20, No. 4, 2027, 8376

($T_{max}$), mass-loss percentages per stage, and final residual char at 800 °C were quantitatively determined.

The bulk crystal structure was observed by X-ray diffraction (XRD) (SmartLab, RIGAKU, Japan). The instrument was operated with Cu-Kα radiation (λ = 1.5418 Å) equipped with a nickel filter. Diffraction patterns were recorded in the 2θ range of 10° to 50° with a step size of 0.02° and a scan speed of 1° per min at room temperature. The relative crystallinity index (CrI) of the samples was quantitatively calculated after baseline subtraction and peak deconvolution using Equation (1) [36]:

$$\text{CrI (\%)} = \frac{I_{110}-I_{am}}{I_{110}} \times 100 \quad (1)$$

where $I_{110}$ is the maximum intensity of the crystalline peak (at $2\theta \approx 22.5°$ for cellulose I) and $I_{am}$ is the intensity of the amorphous diffraction background (at $2\theta \approx 18.0°$.

### 2.5 *Moisture content*

The 2.0 $cm^2$ films were weighed accurately. The films were dried at 110 °C until a fixed dry weight was acquired [37]. The weight of the film at the initial and the dry weight at the final were recorded, and the percentage of moisture content was evaluated as follows Equation (2):

$$\text{Moisture content (\%)} = \frac{W_0-W_f}{W_0} \times 100 \quad (2)$$

where $W_0$ is the weight at the beginning, and $W_f$ is the weight at the final

### 2.6 *Water solubility analysis*

The dried square films of 2.0 $cm^2$ were precisely weighed and recorded. The films were soaked in DI water of 100 mL under stirring at 180 rpm for 6 h at 25 °C [38]. After 6 h, the remaining portions of the film were separated and then dried at 110 °C until constant weight was achieved. The percentage of water solubility was determined as follows Equation (3):

$$\text{Water solubility (\%)} = \frac{W_i-W_f}{W_i} \times 100 \quad (3)$$

where $W_i$ is the weight at the initial stage and $W_f$ is the weight at the final stage.

### 2.7 *Ultraviolet and visible light transmission*

UV-visible light transmission properties of the films were investigated using a UV-Vis spectrophotometer (UV-1280, SHIMADZU, Japan). The film was cut into 4.0 × 1.2 $cm^2$ and placed directly inside the cuvette holder of the spectrophotometer. The transmittance was measured at the wavelength range of 200 - 800 nm. The blocking of UV radiation was calculated as follows Equation (4) [39]:

$$\text{UV-Blocking (\%)} = 100 - T_{UV} \quad (4)$$

where $T_{UV}$ is the average transmittance in the corresponding spectral UV region.

### 2.8 *Biodegradation study*

The film was evaluated using the soil burial test method according to established protocols [40]. Biodegradation of films in soil was carried out for 15 days. Each sample was cut into 2.5 × 2.5 $cm^2$ and was buried to a depth of 10 cm in a soil-filled pot under natural conditions. The test was conducted under controlled laboratory environmental conditions: ambient temperature of 30 °C, relative humidity of 65 %, and soil moisture maintained between 40–50 % by spraying distilled water at regular 24-hour intervals. The pH of the soil matrix was measured at 6.8. The samples were weighed after 2 days. To determine the percentage of biodegradation, the samples were gently removed from the pot and rinsed with DI water. Then, the samples were dried at 50 °C for 24 h and weighed. The percentage of biodegradation was calculated as follows Equation (5):

$$\text{Biodegradation (\%)} = \frac{W_1-W_2}{W_1} \times 100 \quad (5)$$

where $W_1$ is the dry weight at the initial, and $W_2$ is the residue dry weight after biodegradation.

### 2.9 *Statistical analysis*

Experimental measurements were performed in multiple replicates: five specimens (n = 5) were tested for mechanical properties, while three specimens (n = 3) were evaluated for moisture content, water

solubility, and light transmission properties. Data are expressed as the mean ± standard deviation (SD). Statistical evaluation was conducted using one-way Analysis of Variance (ANOVA) followed by Tukey's Honestly Significant Difference (HSD) post-hoc test to determine significant differences between experimental groups. Prior to ANOVA, the normality of data distribution and homogeneity of variances were verified using the Shapiro–Wilk test and Levene's test, respectively. All statistical analyses were executed in SPSS version 26.0. Differences were considered statistically significant at $p$-value < 0.05.

## 3 Results and Discussion

### 3.1 *Surface morphology*

The surface and cross-section morphology of composite films are shown in Figure 2. JSF composite film surface without reinforced BC exhibited roughness, coarseness, irregular patterns, and cracks, whereas JSF/BC-10, JSF/BC-20, JSF/BC-30, JSF/BC-40, and JSF/BC-50 films, which contained BC loading, showed a smooth outer surface without cracks compared with that of the JSF composite film. BC fibers had a uniform dispersion in the starch matrix with no detectable extensive aggregation and agglomeration for the JSF/BC-10, JSF/BC-20, JSF/BC-30, and JSF/BC-40 composite films. However, at 50 wt.% of the BC loading, the JSF/BC-50 revealed aggregation and agglomeration on the surface. This may be attributed to a high cellulose fiber loading, leading to poor dispersion of the cellulose fibers in the starch matrix [41], [42]. The SEM images of the cross-sectional views also showed a uniform incorporation of BC fibers in the starch matrix. Incorporating BC enhances the structural uniformity of the starch layer [43]. Owing to their high compatibility, these BC fibers serve as effective reinforcing agents, facilitating the formation of a continuous matrix without cracks [44]-[46].

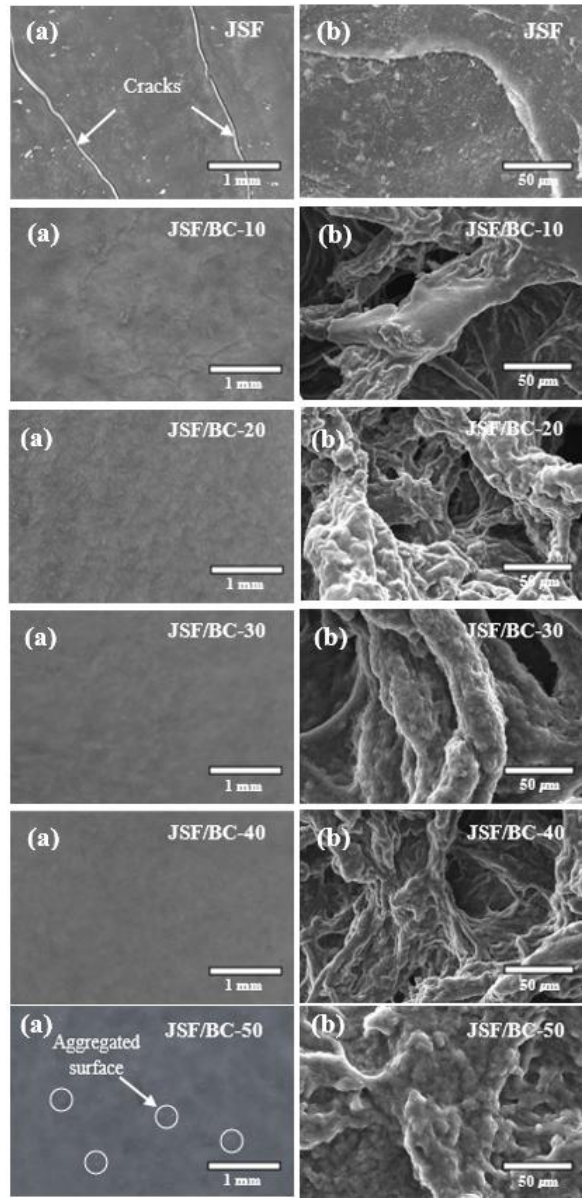



**Figure 2**: SEM images of top (a, x100) and cross-section (b, x2,000) views of films.

### 3.2 *FT-IR analysis*

The chemical characteristics of the films are shown in Figure 3. The FTIR spectra of all samples show a broad band at around 3272 $cm^{-1}$, which is attributed to the O-H stretching vibration of the hydroxyl group. The presence of C-H stretching was also found at 2943 and 2885 $cm^{-1}$. The increase in the intensity of these bands of the JSF/BC composite films can be due to inter- and intra-molecular hydrogen bonding of JSF and BC reinforced into the composite film matrix [47]. The band at 1617 $cm^{-1}$ is attributed to C=O [48]. The adsorption peak at 1000 $cm^{-1}$ can be associated with C–O–C asymmetric stretching of cellulose [49] and starch [50]. It is transformed into two peaks at around 1000 and 995 $cm^{-1}$. This may be because the effect of plasticization by glycerol is associated with the weakening of intramolecular and intermolecular

Applied Science and Engineering Progress, Vol. 20, No. 4, 2027, 8376

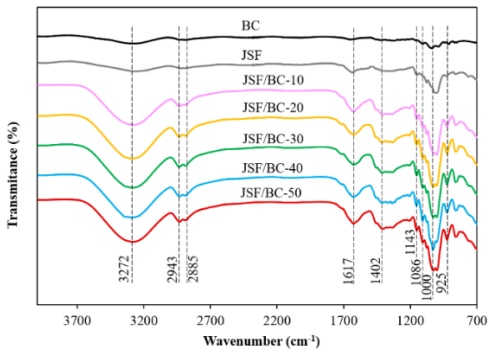



**Figure 3**: FT-IR spectra of films.

hydrogen bonds between the starch chains [51]. It can be seen that this peak becomes more intense after the JSF composite film is reinforced with BC. This peak can be due to the increase in cellulose. The shoulder peaks at 1086 and 925 $cm^{-1}$ are attributed to the stretching of the glucose ring [49]. Additionally, the broad and weak bands appear in the range of 850–700 $cm^{-1}$. This may be associated with out-of-plane bending of bound O-H and C-H deformation frequencies [48]. The observed FTIR patterns indicate the successful preparation of JSF/BC composite film.

### 3.3 *XRD analysis*

The XRD profiles of JSF/BC films are shown in Figure 4. The XRD peaks at 14.1°, 16.1°, and 22.4° are characteristic of the cellulose structure in BC [42], [52]-[54]. The XRD profiles of JSF, JSF/BC-10, JSF/BC-20, JSF/BC-30, JSF/BC-40, and JSF/BC-50 films showed peaks that were located similarly to those of BC. Compared with the XRD profiles of JSF, JSF/BC-10, JSF/BC-20, JSF/BC-30, JSF/BC-40, and JSF/BC-50 films, the peaks of BC were sharp. This indicated that the increase in the amount of BC fiber in the composite film matrix led to an increase in the crystallinity of the composite films [55].

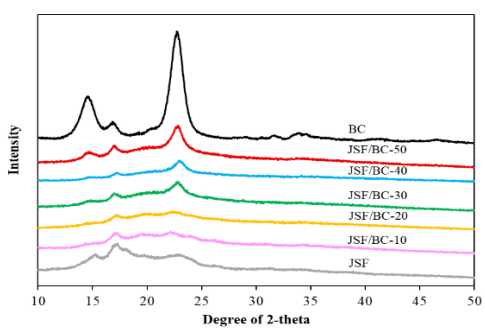



**Figure 4**: XRD pattern of the films.

**Table 1:** Crystallinity index of the films.

| Film | Crystallinity Index (CrI, %) |
|---|---|
| BC | 82.4 |
| JSF | 18.5 |
| JSF/BC-10 | 23.8 |
| JSF/BC-20 | 29.1 |
| JSF/BC-30 | 34.5 |
| JSF/BC-40 | 38.6 |
| JSF/BC-50 | 42.1 |

Incorporating highly crystalline fibers in the amorphous phase of films may introduce localized strains, subsequently facilitating regional crystallization [45], [56]. Quantitative analysis via peak deconvolution demonstrated a progressive increase in the CrI as a function of BC content (Table 1). The CrI increased significantly from 18.5% for pure JSF film to 24.2%, 31.0%, 36.5%, 39.8%, and 42.1% for films loaded with 10, 20, 30, 40, and 50 wt.% BC, respectively. This quantitative rise in CrI confirms the effective integration of highly crystalline BC nanofibrils into the amorphous starch matrix, which directly accounts for the improved mechanical rigidity of the biocomposites.

### 3.4 *Mechanical properties*

The mechanical properties of the composite films are shown in Figure 5. The tensile strength (Figure 5(a)) and elongation (Figure 5(b)) properties of reinforced composite films proved to be superior compared to the non-reinforced composite film. The JSF reinforced with BC was relatively brittle, rigid, and fragile. On the other hand, the tensile strength and elongation of the composite increased with increasing the amount of BC loading, which indicated that the tensile and elongation properties of the composite films reinforced with BC were improved. Statistical analysis using one-way ANOVA with Tukey's HSD post-hoc test ($p$-value < 0.05) confirmed a significant progressive increase in tensile strength and elongation as BC loading increased from 0 to 40 wt.%, peaking at 0.74 MPa and 10.21% at 40 wt.% BC ($p$-value < 0.05). This finding was probably due to the uniform dispersion of cellulose fiber in the film matrix and the formation of intramolecular and intermolecular hydrogen bonding between the cellulose and starch molecules [57]. However, tensile and elongation properties decreased with the amount of BC

loading of 50 wt. % ($p$-value > 0.05), which could be because a higher amount of BC loading of 50 wt.% was not a uniform BC fiber dispersion and distribution, which could lead to an increase in the aggregation and agglomeration, thus decreasing the tensile strength and elongation properties of the films. This result correlates with the SEM observations for the 50 wt.% BC sample, which clearly displayed BC nanofibril bundle aggregation, localized voids, and interfacial phase discontinuities. Excessive BC concentration induces self-entanglement of nanofibrils via strong inter-particle hydrogen bonding, exceeding the wetting capacity of the JSF matrix [58]. These aggregated fiber clusters act as internal stress concentration sites that facilitate premature crack initiation under mechanical load, explaining the observed drop in tensile strength and film ductility [58]. The result suggested that the BC enhanced the mechanical properties of composite films. The JSF/BC-40 with the BC loading of 40 wt.% exhibited the highest tensile strength and elongation of 0.74 MPa and 10.21%, respectively.

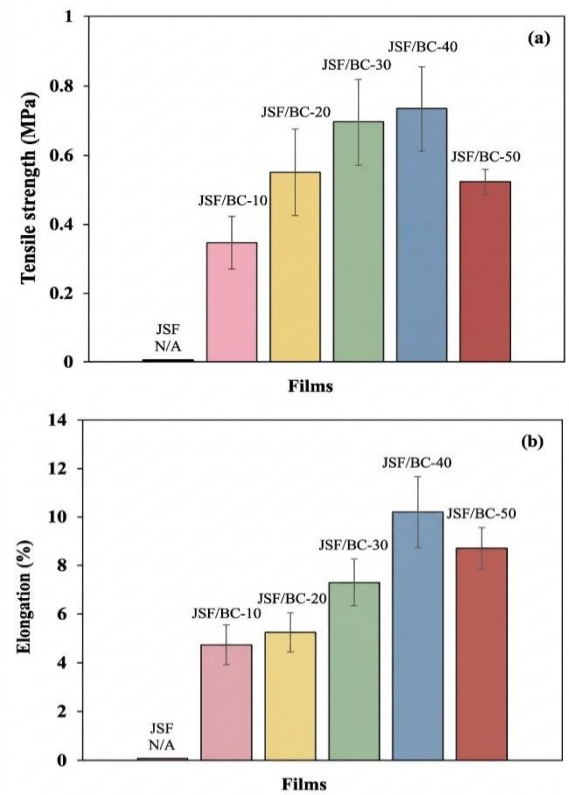



**Figure 5**: a) Tensile strength and b) elongation properties of films.

Although this represents a notable enhancement compared to the unreinforced JSF film, the maximum TS of 0.74 MPa remains significantly lower than that of conventional petro-based packaging plastics, such as low-density polyethylene (LDPE, 10–30 MPa) [59] or polypropylene (PP, 25–40 MPa) [60], as well as high-performance starch biocomposites reported in the literature [51], [61]. This difference in mechanical resistance is primarily attributed to the hydrophilic nature of starch and the absence of strong covalent crosslinking within the matrix [62]. Consequently, the prepared JSF/BC films are not intended to replace synthetic polymers in heavy-duty structural packaging or high-load applications.

Nevertheless, a tensile strength of 0.74 MPa, combined with the inherent flexibility imparted by glycerol, falls within an acceptable range for specific light-duty, short-term, and single-use eco-packaging applications [63]. Potential target applications include biodegradable food overwraps for dry products, agricultural mulch films, disposable lining sheets, or inner protective sachets where rapid environmental degradation and compostability are prioritized over high load-bearing capacity [63], [64]. Future work may focus on incorporating bio-based crosslinking agents or surface chemical modifications to further boost the interfacial bonding and mechanical performance to meet broader commercial packaging requirements.

### 3.5 *Thermal stability*

The mass loss profile during thermal gravimetric analysis of composite films is shown in Figure 6 and Table 2. The profiles show that the trends of the TGA patterns of all composite films are similar. The initial mass loss at temperatures around 50 °C up to 110 °C could be described as the elimination of moisture in the composite film structure, which was approximately 5% of the initial weight. The mass loss at temperatures around 110 °C up to 280 °C was associated with the volatilization and thermal degradation of the glycerol plasticizer and initial starch depolymerization [65]. BC showed a decomposition temperature range between 300 and 380 °C while the JSF composite film had a decomposition temperature range between 200 and 350 °C. The result showed that the BC had higher thermal stability than the JSF composite film. This is because the BC had high crystallinity. The decomposition of the JSF/BC composite films showed a decomposition temperature range from 280 to 380 °C. It slightly shifted to a higher decomposition temperature compared with

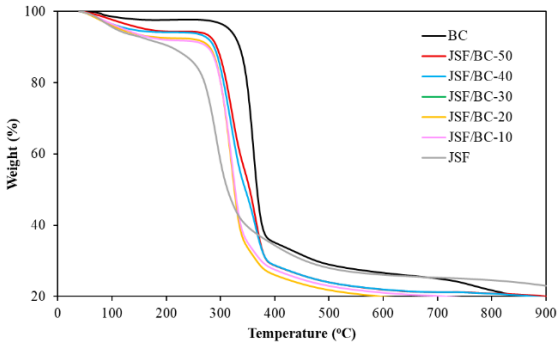



**Figure 6**: TGA thermograms of films.

that of JSF composite films. The incorporation of BC nanofibrils progressively shifted $T_{onset}$ from 265 °C (pure JSF) to 288 °C (50 wt.% BC). Similarly, the main decomposition peak ($T_{max2}$) increased from 315 °C to 340 °C, demonstrating enhanced thermal stability imparted by the highly crystalline BC nanofiber network [66]. The final residual mass at 800 °C also increased from 12.1% to 22.4% with higher BC loading due to higher carbonization of cellulose fibers [66].

The thermal stability of JSF/BC composite films follows the order: JSF/BC-50 > JSF/BC-40 > JSF/BC-30 > JSF/BC-20 > JSF/BC-10, which could indicate that the increase in the amount of BC in the JSF/BC composite films enhances the thermal stability. This thermal enhancement can be primarily attributed to two complementary mechanisms: (1) interfacial molecular immobilization, in which extensive hydrogen bonding between the hydroxyl groups of BC and the hydroxyl-rich chains of gelatinized JSF restricts polymer-chain mobility and enhances interfacial cohesion; and (2) the highly ordered crystalline structure of BC, which contributes to its intrinsic thermal stability and consequently improves the resistance of the composite matrix to thermal degradation [67]-[69].

Previous studies have demonstrated that the incorporation of BC or nanocellulose into starch-based matrices can improve thermal stability through strong polymer and cellulose interactions and the formation of dense cellulose networks [67], [68]. Nunes *et al.,* reported that the thermal stability of JSF/BC biocomposites was strongly influenced by composition and attributed the relatively high thermal stability of BC to its high crystallinity and purity, while the addition of BC to starch was associated with improved thermal stability arising from the high thermal stability of cellulose and the compatibility between starch and cellulose [67]. Similarly, recent work on JSF/BC biocomposite films demonstrated that increasing nanocellulose loading enhanced thermal stability, together with increased hydrogen bonding and crystallinity within the composite matrix [68], [69]. The thermal stability of BC itself has also been associated with its crystalline structure, molecular characteristics, and hydrogen-bonded network [69]. Accordingly, the TGA results obtained in the present study indicate that the incorporation of BC enhanced the thermal resistance of the JSF/BC films. However, the upper processing temperature should be selected below the onset of significant thermal degradation rather than being defined solely by the nominal temperature range of the TGA profile.

### 3.6 *Moisture content and water solubility*

The water-resistant properties are presented in Figure 7. The JSF without BC reinforcement had the highest water uptake. The moisture uptake (Figure 7(a)) decreased with the increase in the BC loading, which

**Table 2:** Thermal degradation parameters, degradation stages, and mass loss percentages of films.

| Sample | $T_{onset}$ (°C) | $T_{max1}$ (°C) | $T_{max2}$ (°C) | Mass-loss stages (%) | | | Final residue at 800 °C (%) |
|---|---|---|---|---|---|---|---|
| | | | | 50–110 °C | 110–280 °C | 280–380 °C | |
| BC | 305 | — | 348 | 4.1 | — | 71.5 | 24.4 |
| JSF | 265 | 215 | 315 | 8.2 | 22.5 | 57.2 | 12.1 |
| JSF/BC-10 | 271 | 218 | 322 | 7.8 | 21.0 | 56.7 | 14.5 |
| JSF/BC-20 | 276 | 221 | 328 | 7.1 | 19.8 | 56.3 | 16.8 |
| JSF/BC-30 | 280 | 223 | 334 | 6.5 | 18.2 | 56.4 | 18.9 |
| JSF/BC-40 | 285 | 225 | 338 | 5.9 | 17.0 | 56.4 | 20.7 |
| JSF/BC-50 | 288 | 226 | 342 | 5.4 | 15.8 | 56.4 | 22.4 |

follows the order: 25.7%, 19.6%, 17.5%, 13.3%, 11.9%, and 8.5% for JSF, JSF/BC-10, JSF/BC-20, JSF/BC-30, JSF/BC-40, and JSF/BC-50, respectively. Similarly, the addition of BC to the JSF matrix also contributed to reducing water solubility (Figure 7(b)), following the order: 32.1%, 26.6%, 23.0%, 17.8%, 16.6%, and 10.9% for JSF, JSF/BC-10, JSF/BC-20, JSF/BC-30, JSF/BC-40, and JSF/BC-50, respectively. These can be described as the formation of a starch/BC network by hydrogen bonding between the BC and the hydroxyl groups of the starch matrix, which interacts between cellulose and starch chains, leading to restricted entry of water molecules [49], [50]. The result suggested that the reinforcement of JSF composite film with BC can enhance moisture resistance and water solubility.

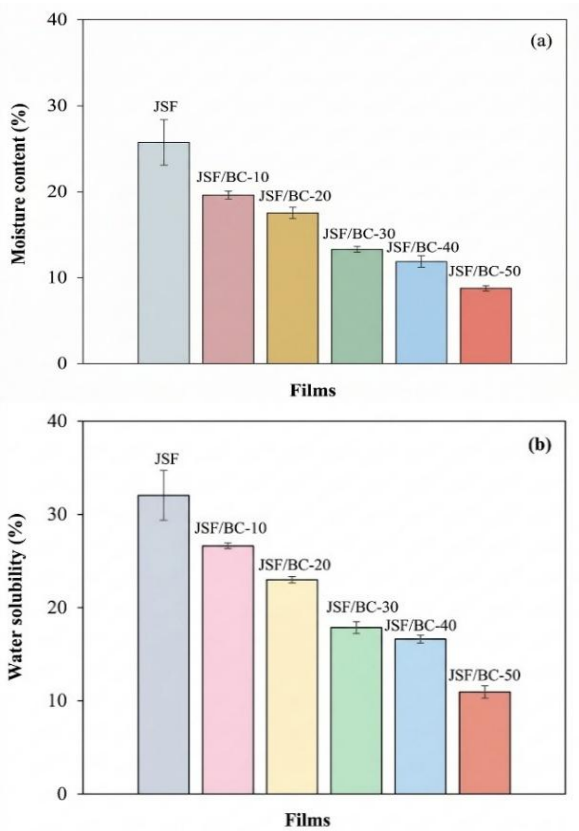



**Figure 7**: Moisture content a) and water solubility b) of the composite films.

### 3.7 *Ultraviolet and visible light transmission*

To observe the effective UV-shielding capacity, the transmission of UV-visible light through the composite films was studied as shown in Figure 8(a). All composite films exhibited total blockage of UV light up to 340 nm. However, the JSF exhibited the highest UV light transmission compared to other composite films, indicating low UV-shielding capability. Meanwhile, the JSF/BC composite films showed a lower UV-Vis light transmission compared with JSF. A reduction in transmittance corresponds to increased opacity, effectively serving as an excellent barrier to light-induced lipid oxidation [70]. From transmittance spectra in the range of 200-340 nm, the UV radiation blocking was calculated as shown in Figure 8(b). The UV radiation blocking ability of composite films increased with increasing the amount of BC loading, which was 65.8%, 68.8%, 76.6%, 83.7%, 88.1%, and 91.1% for JSF, JSF/BC-10, JSF/BC-20, JSF/BC-30, JSF/BC-40, and JSF/BC-50, respectively. The result confirmed that the increase in BC loading significantly enhanced the UV radiation blocking ability, possibly by increasing the density and viscosity of the composite films [71].

### 3.8 *Biodegradation study*

The tests resemble actual conditions by embedding composite films in soil, facilitating the gradual decomposition of the material by soil microorganisms [72]. The weight loss during biodegradation of composite films is shown in Figure 9. The degradation rates of all samples rapidly increased in the initial (0 – 3 days), and then the degradation rates slowly decreased. This is because the surface layer of the composite films was predominantly decomposed by microorganisms in the soil [73]. The starch and other organic substances were inhibited by the microorganisms, resulting in a fast decomposition rate in the early phase within 3 days. Overall, more than 70% of the composite films were biodegradable within 15 days. The JSF and JSF/BC-10 achieved the highest decomposition of 100% within 5 and 11 days, respectively. Meanwhile, decompositions of JSF/BC-20, JSF/BC-30, JSF/BC-40, and JSF/BC-50 were 98.8%, 89.2%, 81.0%, and 72.1% within 15 days, respectively. The results showed that the decomposition decreased with an increase in the BC loading.

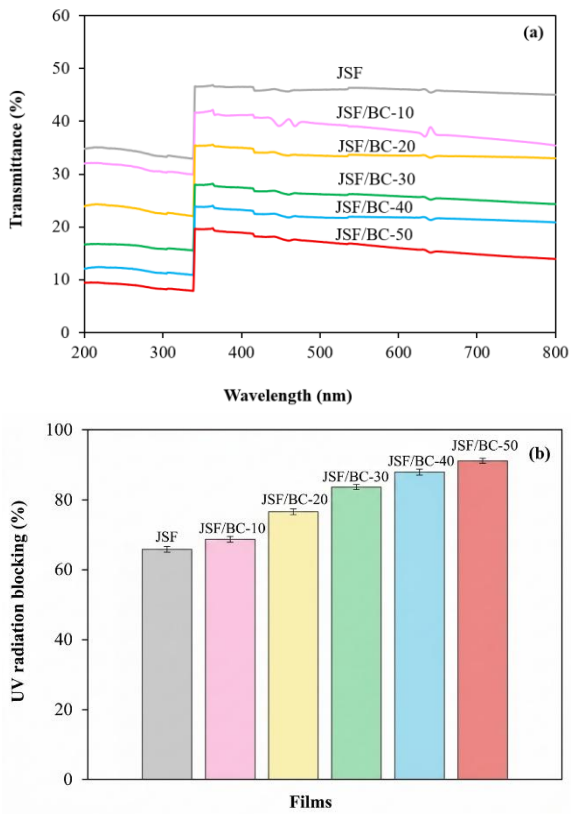



**Figure 8**: The UV-Vis a) light transmission and b) radiation blocking of films.

The reason might be that the increase in the BC loading enhances the composite film structure, which takes longer time to decompose. All composite films developed in this study showed significantly high biodegradability, environmental friendliness, and sustainability.

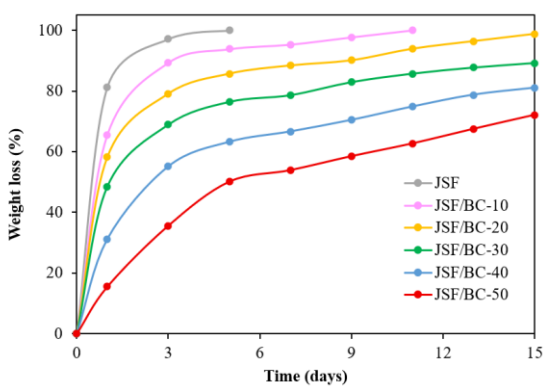



**Figure 9**: Biodegradability of the composite films.

### 3.9 *Comparative evaluation and applications*

To comprehensively benchmark the performance of the JSF/BC composite film against a broader range of commercial and research packaging materials, Table 3 provides an expanded comparative overview encompassing conventional petro-based plastics (LDPE, PP, and PET), biodegradable synthetic polymers and their blends (PLA and PBAT/starch), and modified biopolymer systems (corn starch/chitosan and cassava starch/BC). Conventional petro-based plastics generally exhibit substantially higher mechanical strength and lower moisture sensitivity than starch-based films, while PLA- and PBAT-based materials provide improved mechanical and barrier performance compared with unmodified starch films [74], [75].

As shown in Table 3, the JSF/BC-40 film exhibited a maximum tensile strength of 0.74 MPa and an elongation at break of 10.21%, indicating a balance between flexibility and structural integrity suitable for low-stress packaging applications. In comparison, starch–chitosan films have demonstrated improved mechanical and UV-barrier properties through polymer–polymer interactions, while cassava starch/bacterial cellulose bioplastics have shown increased tensile strength with increasing BC content [76], [77]. The relatively lower tensile strength of JSF/BC-40 may therefore reflect the inherently hydrophilic and relatively weakly interacting nature of the starch-rich matrix, despite the reinforcing contribution of the BC network.

Importantly, the incorporation of BC provides functional advantages beyond mechanical reinforcement. Bacterial cellulose possesses a highly interconnected nanofibrous network and has demonstrated excellent UV-barrier properties, making BC-containing films particularly attractive for packaging applications where protection against light-induced deterioration is required [78]. The JSF/BC-40 film exhibited 88.1% UV shielding and thermal stability up to approximately 270 °C, suggesting that the BC network contributed to both optical shielding and thermal resistance. Similar improvements in functional and barrier properties have been reported for cellulose-reinforced biopolymer films, including starch–bacterial cellulose and other polysaccharide-based packaging systems [77]-[79].

Therefore, although the tensile strength of JSF/BC-40 remains substantially lower than that of conventional petro-based packaging plastics and high-

**Table 3:** Comparative property overview of JSF/BC biocomposite film against conventional synthetic plastics and various reported biopolymer packaging films.

| Film | Tensile Strength (MPa) | Elongation at Break (%) | UV-Blocking Capability (%) | Biodegradability | Ref. |
|---|---|---|---|---|---|
| JSF/BC-40 | 0.74 | 10.21 | 88.1 | 72.1–100% | This study |
| LDPE | 10–30 | 100–600 | Low | Non-biodegradable | [74] |
| PP | 25–40 | 200–600 | Low | Non-biodegradable | [74] |
| PET | 50–80 | 50–300 | Moderate | Non-biodegradable | [74] |
| PLA | 40–70 | 2–10 | Moderate | Industrial composting | [74],[75] |
| PBAT | 15–40 | 400–700 | Low–moderate | Biodegradable | [74],[75] |
| Corn starch/chitosan | ~2–10 | ~10–30 | High | Biodegradable | [76] |
| Cassava starch/BC | 2.34 | — | — | Biodegradable | [77] |
| Thermoplastic starch/BNC | ~23–39 | — | — | Biodegradable | [78] |
| Potato starch nanocomposite | 53.6 | — | High | Biodegradable | [79] |

performance biodegradable polymer films, its combination of biodegradability, UV shielding, and thermal resistance provides potential for light-duty and short-term packaging applications, particularly for dry-food packaging, inner liners, protective wraps, and secondary agricultural packaging. The present material should therefore be regarded as a functional biodegradable packaging candidate rather than a direct replacement for high-strength structural packaging plastics.

### 3.10 *Environmental significance and sustainability outlook*

Beyond its structural and functional properties, the JSF/BC biocomposite system holds substantial environmental significance. Jackfruit seed flour (JSF), an underutilized starch-rich agricultural byproduct, serves as a low-cost, renewable matrix, aligning directly with agricultural waste valorization principles [80]. The integration of microbial bacterial cellulose (BC) further enhances material performance without relying on synthetic chemical additives. From a circular economy perspective, converting tropical fruit waste into functional bio-packaging reduces agro-industrial disposal burdens and reliance on fossil resources [78], [80].

Compared to conventional petroleum-based packaging plastics such as Low-Density Polyethylene (LDPE) and Polypropylene (PP). JSF/BC biocomposite films offer complete biodegradability and carbon neutrality [78], [81]. These ecological attributes render JSF/BC biocomposite films a promising, sustainable alternative for single-use flexible inner food wraps, supporting global initiatives to replace non-biodegradable synthetic plastics with eco-friendly bio-based materials.

## 4 Conclusion

This study successfully developed and characterized JSF/BC composite films reinforced with BC. SEM analysis exhibited that BC fibers in slurry form at 10 - 50 wt.% (wet basis) loading contents were uniformly dispersed and distributed within the starch matrix, which revealed that the JSF/BC-40 at a BC loading of 40 wt.% achieved optimal dispersion. Structural analysis through FT-IR and XRD also verified the interaction of BC within the starch matrix, contributing to improved film integrity. Mechanical analysis revealed that the BC improved tensile strength and elongation. The JSF/BC-40 had the highest tensile strength of 0.74 MPa and elongation of 10.21%. Furthermore, TGA analysis also shows that the incorporation of BC in the starch matrix enhances

the thermal properties. All JSF/BC composite films had thermal stability at temperatures up to approximately 270 °C. The moisture content and water content decreased with the increase in BC loading. UV-Visible analysis revealed that the JSF/BC composite films enhanced UV-protection ability by 65.8 - 91.1%. Additionally, the biodegradability of the JSF/BC composite films was 72.1 - 100%, and it was achieved in 15 days. Because of its excellent properties, the JSF/BC composite films are expected to have high potential uses as packaging and short-term packaging. These findings demonstrate that the developed composite film has a high potential for sustainable packaging, highlighting the potential of agricultural waste for high performance, which aligns with circular economy principles. While this study establishes the structural and mechanical optimization of JSF/BC biocomposite films, current limitations include the lack of direct oxygen permeability profiling and real-time food shelf-life storage trials, which are designated as key priorities for future applied packaging evaluations. Future work will focus on evaluation of oxygen permeability, water vapor permeability, contact angle, transparency, and food storage performance.

## Acknowledgments

This research was funded by King Mongkut's University of Technology North Bangkok, Contract no. KMUTNB-67-NEW-06.

## Author Contributions

A.K., T.C., and T.P.: Data curation, Formal analysis, Investigation, Methodology, Software, Visualization, Writing – original draft; A.K. and S.P.: Formal analysis, Investigation; S.P. and V.P: Resources, Validation; A.K.: Conceptualization, Funding acquisition, Investigation, Methodology, Project administration, Resources, Supervision, Validation, Visualization, Writing – review & editing.

## Conflicts of Interest

The authors declare no conflict of interest.

## Declaration of generative AI and AI-assisted technologies in the writing process

The authors utilized the ChatGPT tool to enhance the language and readability of the manuscript.

## References

[1] A. S. Ratna, C. Verma, S. Hossain, B. Gupta, and S. Mukhopadhyay, "Development of corn husk cellulose reinforced polyvinyl alcohol bio-composite films incorporated with Zinc Oxide nanoparticles," *Bioresource Technology Reports*, vol. 23, Sep. 2023, Art. no. 101570, doi: 10.1016/j.biteb.2023.101570.

[2] W. Dai, Y. Lan, Y. Wang, and H. Xu, "Bioplastics vs. conventional plastics: Degradation pathways, ecotoxicological impact and exposure health risks," *Journal of Environmental Chemical Engineering*, vol. 13, no. 6, Dec. 2025, Art. no. 120397, doi: 10.1016/j.jece.2025.120397.

[3] A. A. Kacaribu, Rahmi, Julinawati, H. Fathana, M. Reza, and M. Iqhramullah, "Preparation and characterization of cellulose film from velvet tamarind rind (*Dialium indum* L.) for food packaging," *Applied Science and Engineering Progress*, vol. 18, no. 3, 2025, Art. no. 7724, doi: 10.14416/j.asep.2025.03.006.

[4] N. M. Aguilar, F. Arteaga-Cardona, M. E. de Anda Reyes, J. J. Gervacio-Arciniega, and U. Salazar-Kuri, "Magnetic bioplastics based on isolated cellulose from cotton and sugarcane bagasse," *Materials Chemistry and Physics*, vol. 238, Dec. 2019, Art. no. 121921, doi: 10.1016/j.matchemphys.2019.121921.

[5] R. Poudel, N. Dutta, and N. Karak, "A mechanically robust biodegradable bioplastic of citric acid modified plasticized yam starch with anthocyanin as a fish spoilage auto-detecting smart film," *International Journal of Biological Macromolecules*, vol. 242, Jul. 2023, Art. no. 125020, doi: 10.1016/j.ijbiomac.2023.125020.

[6] H. Zhang et al., ""Brick-and-Mortar" multidimensional sodium alginate composite films reinforced with ginger residue nanocellulose for high-performance biodegradable packaging," *Journal of Environmental Chemical Engineering*, vol. 14, Apr. 2026, Art. no. 122076, doi: 10.1016/j.jece.2026.122076.

[7] S. Phomrak and M. Phisalaphong, "Lactic acid modified natural rubber–bacterial cellulose composites," *Applied Sciences*, vol. 10, no. 10, 2020, Art. no. 3583, doi: 10.3390/app10103583.

[8] E. M. A. Hamid et al., "Optimization of corn starch/glycerol, acetic acid, and cellulose fibers ratio on biodegradable plastic synthesis by Box–Behnken design (BBD)," *Clean Technologies and Environmental Policy*, vol. 27, pp. 4433–4455, Sep. 2025, doi: 10.1007/s10098-025-03135-7.

[9] Y. Zhou et al., "A printed, recyclable, ultra-strong, and ultra-tough graphite structural material," *Materials Today*, vol. 30, pp. 17–25, Nov. 2019, doi: 10.1016/j.mattod.2019.03.016.

[10] C. Jia et al., "From wood to textiles: Top-down assembly of aligned cellulose nanofibers," *Advanced Materials*, vol. 30, no. 30, Jul. 2018, Art. no. 1801347, doi: 10.1002/adma.201801347.

[11] M. Zhu et al., "Anisotropic, transparent films with aligned cellulose nanofibers," *Advanced Materials*, vol. 29, no. 21, Jun. 2017, Art. no. 1606284, doi: 10.1002/adma.201606284.

[12] B. Pfister et al., "Recreating the synthesis of starch granules in yeast," *eLife*, vol. 5, 2016, Art. no. e15552, doi: 10.7554/eLife.15552.

[13] M. Talha et al., "Valorization of *Musa paradisiaca* peel waste for bioplastic production: a study on microbial degradation dynamics," *Waste and Biomass Valorization*, vol. 17, pp. 2019–2028, Apr. 2026, doi: 10.1007/s12649-025-03228-w.

[14] A. Anbalagan et al., "Development and optimization of sustainable sisal fibre/karaya gum reinforced polyester composites: Mechanical, thermal, dielectric and moisture absorption performance," *Next Materials*, vol. 13, Oct. 2026, Art. no. 102568, doi: 10.1016/j.nxmate.2026.102568.

[15] P. Prabhu et al., "Natural gum integrated polymer composites: A study of mechanical, water absorption, visco-elastic and dielectric properties," *Next Materials*, vol. 12, Jul. 2026, Art. no. 102113, doi: 10.1016/j.nxmate.2026.102113.

[16] D. Booramurthy, P. Sreenivas, S. L. P. Kumar, B. Paramasivam, and M. Sriariyanun, "Cryogenic-treated surface-modified hybrid nanofillers for enhanced mechanical performance and thermal stability of epoxy nanocomposites," *Next Materials*, vol. 13, Oct. 2026, Art. no. 102890, doi: 10.1016/j.nxmate.2026.102890.

[17] B. Paramasivam, E. Uthirapathi, S. Malinee, and B. N. Shanmugam, "Evaluating the effect of discarded tube light particle filler on the mechanical performance of epoxy/novel crown root fiber bio-composites," *Materials Science and Technology*, 2026, doi: 10.1177/02670836261444116.

[18] M. Sriariyanun, K. Koppiahraj, P. Baranitharan, K. Rajeshkumar, and V. Kavimani, "Optimization of mechanical properties for bio-filler embedded bio-composites using hybrid optimization techniques," *Environmental Progress & Sustainable Energy*, vol. 45, no. 1, 2026, Art. no. e70165, doi: 10.1002/ep.70165.

[19] P. Baranitharan, U. Elaiyarasan, M. Sriariyanun, S. Venkatesh, and N. S. Balaji, "Sustainable bio-composites from agro-green waste: Optimize the effect of waste ceramic particles filler addition on mechanical performance," *Environmental Progress & Sustainable Energy*, 2026, Art. no. e70556, doi: 10.1002/ep.70556.

[20] T. K. Nguyen, N. T. T. That, N. T. Nguyen, and H. T. Nguyen, "Development of starch-based bioplastic from Jackfruit seed," *Advances in Polymer Technology*, 2022, Art. no. 6547461, doi: 10.1155/2022/6547461.

[21] A. Kaitheri et al., "Synthesis and characterisation of titania supported on bacterial cellulose films and evaluation of photocatalytic activity under solar irradiation," *Journal of Environmental Chemical Engineering*, vol. 13, no. 3, Jun. 2025, Art. no. 116976, doi: 10.1016/j.jece.2025.116976.

[22] P. Jaroenjaturong, B. Cheirsilp, U. Thumarat, and P. Boonsawang, "Enhanced bacterial nano-cellulose production by *Acetobacter xylinum* using cost-effective sweet black tea medium added with ethanol," *Bioresource Technology Reports*, vol. 33, Feb. 2026, Art. no. 102482, doi: 10.1016/j.biteb.2025.102482.

[23] L. T. Khanh Vu, A. T. Kim Nguyen, and N. L. Le, "Activity and stability of lipases immobilized onto acetylated bacterial cellulose," *Applied Science and Engineering Progress*, vol. 16, no. 4, 2023, Art. no. 6812, doi: 10.14416/j.asep.2023.04.002.

[24] Q.-D. Nguyen, T.-V.-L. Nguyen, T.-T.-D. Nguyen, and N.-N. Nguyen, "Effects of different hydrocolloids on the production of bacterial cellulose by *Acetobacter xylinum* using Hestrin–Schramm medium under anaerobic condition," *Bioresource*

*Technology Reports*, vol. 17, Feb. 2022, Art. no. 100878, doi: 10.1016/j.biteb.2021.100878.

[25] C. Saejung, N. Thaoto, and A. Chaiyarat, "Molasses-grown bacterial cellulose as a filter membrane to filter bacteria, wastewater, and oil," *Waste and Biomass Valorization*, vol. 16, pp. 2391–2403, May 2025, doi: 10.1007/s12649-024-02826-4.

[26] S. S. Ting, G. P. Gie, M. F. Omar, and M. F. Abdullah, "Nanocellulose-reinforced biocomposites," *Biomass, Biofuels, Biochemicals*, pp. 461-494, 2021, doi: 10.1016/B978-0-12-821888-4.00016-2.

[27] B. Paramanathan et al., "Microbial fabrication of selenium nanoparticles and bacterial cellulose-SeNPs nanocomposite for multifunctional applications," *Materials Chemistry and Physics*, vol. 350, Feb. 2026, Art. no. 131891, doi: 10.1016/j.matchemphys.2025.131891.

[28] P. P. Phatchayawat, S. Yodmuang, and M. Phisalaphong, "Bacterial nanocellulose-chitosan-gelatin-hydroxyapatite scaffolds for bone tissue engineering," *Macromolecular Bioscience*, vol. 25, no. 11, Nov. 2025, Art. no. e00299, doi: 10.1002/mabi.202500299.

[29] A. Khamkeaw, T. Asavamongkolkul, T. Perngyai, B. Jongsomjit, and M. Phisalaphong, "Interconnected micro, meso, and macro porous activated carbon from bacterial nanocellulose for superior adsorption properties and effective catalytic performance," *Molecules*, vol. 25, no. 18, 2020, Art. no. 4063, doi: 10.3390/molecules25184063.

[30] A. Windarsih et al., "Gold modified bacterial cellulose from coconut water waste and its antibacterial activity," *Waste and Biomass Valorization*, vol. 13, pp. 4157–4164, Oct. 2022, doi: 10.1007/s12649-022-01769-y.

[31] S. Phomrak, A. Nimpaiboon, B.-m. Z. Newby, and M. Phisalaphong, "Natural rubber latex foam reinforced with micro- and nanofibrillated cellulose via Dunlop method," *Polymers*, vol. 12, no. 9, 2020, Art. no. 1959, doi: 10.3390/polym12091959.

[32] S. Phomrak and M. Phisalaphong, "Reinforcement of natural rubber with bacterial cellulose via a latex aqueous microdispersion process," *Journal of Nanomaterials*, 2017, Art. no. 4739793, doi: 10.1155/2017/4739793.

[33] A. Almi, R. A. Ilyas, M. A. M. Rizal, and M. Mahardika, "Recent advances and developments of nanocellulose reinforced thermoplastic starch bionanocomposite: A review," *ChemBioEng Reviews*, vol. 13, no. 2, Apr. 2026, Art. no. e70055, doi: 10.1002/cben.70055.

[34] A. Dhatwalia, K. Sood, R. Saini, and A. Dhiman, "Jackfruit seed starch (JFSS): extraction, structural properties, functional modifications, and applications in food systems—a review," *Journal of Food Measurement and Characterization*, vol. 20, pp. 14788–14814, Aug. 2026, doi: 10.1007/s11694-026-04657-4.

[35] R. F. Santana et al., "Characterization of starch-based bioplastics from jackfruit seed plasticized with glycerol," *Journal of Food Science and Technology*, vol. 55, pp. 278–286, Jan. 2018, doi: 10.1007/s13197-017-2936-6.

[36] M. S. Jafari, S. Ghadami, S. Mantripragada, K. Dellinger, J. R. Alston, and D. R. LaJeunesse, "Facile and green carboxylation of never-dried bacterial cellulose produced from low-cost substrates: structural characterization and copper binding performance," *Materials Advances*, vol. 6, no. 23, pp. 8936–8951, Dec. 2025, doi: 10.1039/d5ma00725a.

[37] M. K. Marichelvam, M. Jawaid, and M. Asim, "Corn and rice starch-based bio-plastics as alternative packaging materials," *Fibers*, vol. 7, no. 4, 2019, Art. no. 32, doi: 10.3390/fib7040032.

[38] R. U. Mahmud, M. A. Darda, M. T. Hossain, M. A. Habib, R. K. Nag, and M. P. Sarker, "Fabrication of waste cotton reinforced corn and potato starch sustainable bioplastics for eco-friendly packaging material," *Sustainable Chemistry for the Environment*, vol. 11, Sep. 2025, Art. no. 100286, doi: 10.1016/j.scenv.2025.100286.

[39] S. Guzman-Puyol et al., "Transparent, UV-blocking, and high barrier cellulose-based bioplastics with naringin as active food packaging materials," *International Journal of Biological Macromolecules*, vol. 209, pp. 1985–1994, Jun. 2022, doi: 10.1016/j.ijbiomac.2022.04.177.

[40] K. Chaisuwan, D. Anurakumphan, S. Hemmanee, J. Ruamcharoen, and M. Leelakriangsak, "Soil burial degradation of starch-based films on microbial load and plant growth," *Journal of Sustainability Science and Management*, vol. 18, no. 3, pp. 110–124, Mar. 2023, doi: 10.46754/jssm.2023.03.008.

[41] J. F. F. Macena, J. C. A. de Souza, G. P. Camilloto, and R. S. Cruz, "Physico-chemical, morphological and technological properties of the avocado (*Persea americana* Mill. cv. Hass) seed starch," *Ciência e Agrotecnologia*, vol. 44, 2020, Art. no. e001420, doi: 10.1590/1413-7054202044001420.

[42] B. Saha, A. Sathyan, P. Singh, A. S. Kalamdhad, and M. Khwairakpam, "Prerequisite of electrohydrolysis pretreatment on lignocellulose terrestrial weed (*Ageratum conyzoides*) to enhance the methane production and continuous reactor study," *Materials Science for Energy Technologies*, vol. 3, pp. 896–904, 2020, doi: 10.1016/j.mset.2020.10.006.

[43] B. Saha, S. Koley, M. Khwairakpam, and A. S. Kalamdhad, "Comparative study between mono-digestion and co-digestion of terrestrial weed (*Parthenium hysterophorus*)," *Cleaner Engineering and Technology*, vol. 11, Dec. 2022, Art. no. 100560, doi: 10.1016/j.clet.2022.100560.

[44] B. Saha et al., "Optimising biogas production from *Parthenium hysterophorus* biomass through thermal pretreatment and batch anaerobic digestion," *Fermentation*, vol. 12, no. 3, 2026, Art. no. 135, doi: 10.3390/fermentation12030135.

[45] B. Saha, A. S. Kalamdhad, and M. Khwairakpam, "Efficiency of electrohydrolysis pretreatment on terrestrial weed (*Parthenium hysterophorus*) to cut down the hydrolysis stage during the anaerobic digestion process and continuous reactor study," *Energy Reports*, vol. 7, pp. 3547–3555, Nov. 2021, doi: 10.1016/j.egyr.2021.06.023.

[46] F. Hidayat, A. Noviyanti, Rahmi, E. Indarti, S. Nurman, and A. Anta Kacaribu, "Development of kimpul Starch-Based composite films reinforced with TEMPO-oxidized cellulose microfiber for food packaging," *Applied Science and Engineering Progress*, vol. 19, no. 4, 2026, Art. no. 8101, doi: 10.14416/j.asep.2026.04.001.

[47] M. Islam, A. S. K. Sinha, and K. Prasad, "PLA/starch bi-layer films reinforced with rice straw cellulose nanofibers and functionalized with organosolv–lignin nanoparticles and grapefruit bioactives for shelf life extension of green grapes," *Sustainable Food Technology*, vol. 4, no. 1, pp. 752–771, Sep. 2025, doi: 10.1039/d5fb00561b.

[48] Maryam et al., "Characteristics of food packaging bioplastics with nanocrystalline cellulose (NCC) from oil palm empty fruit bunches (OPEFB) as reinforcement," *Journal of Renewable Materials*, vol. 13, no. 12, pp. 2431–2451, Dec. 2025, doi: 10.32604/jrm.2025.02024-0063.

[49] M. B. Agustin, B. Ahmmad, S. M. M. Alonzo, and F. M. Patriana, "Bioplastic based on starch and cellulose nanocrystals from rice straw," *Journal of Reinforced Plastics and Composites*, vol. 33, no. 24, pp. 2205–2213, 2014, doi: 10.1177/0731684414558325.

[50] K. J. Falua, A. Babaei-Ghazvini, and B. Acharya, "Characterization and environmental footprint of crosslinked faba bean starch-based ecofilms reinforced with tunicate cellulose nanocrystals," *Sustainable Materials and Technologies*, vol. 43, Apr. 2025, Art. no. e01236, doi: 10.1016/j.susmat.2025.e01236.

[51] T. Almeida et al., "Biobased ternary films of thermoplastic starch, bacterial nanocellulose and gallic acid for active food packaging," *Food Hydrocolloids*, vol. 144, Nov. 2023, Art. no. 108934, doi: 10.1016/j.foodhyd.2023.108934.

[52] L. Hong, Y. L. Wang, S. R. Jia, Y. Huang, C. Gao, and Y. Z. Wan, "Hydroxyapatite/bacterial cellulose composites synthesized via a biomimetic route," *Materials Letters*, vol. 60, no. 13–14, pp. 1710–1713, Jun. 2006, doi: 10.1016/j.matlet.2005.12.004.

[53] S. Keshk and K. Sameshima, "Influence of lignosulfonate on crystal structure and productivity of bacterial cellulose in a static culture," *Enzyme and Microbial Technology*, vol. 40, no. 1, pp. 4–8, Dec. 2006, doi: 10.1016/j.enzmictec.2006.07.037.

[54] M. Phisalaphong and N. Jatupaiboon, "Biosynthesis and characterization of bacteria cellulose–chitosan film," *Carbohydrate Polymers*, vol. 74, no. 3, pp. 482–488, Nov. 2008, doi: 10.1016/j.carbpol.2008.04.004.

[55] W. Somphol et al., "Extraction of cellulose nanocrystals and nanofibers from rubber leaves and their impacts on natural rubber properties," *Applied Science and Engineering Progress*, vol. 17, no. 2, 2024, Art. no. 7281, doi: 10.14416/j.asep.2023.11.010.

[56] A. Sonia and K. P. Dasan, "Celluloses microfibers (CMF)/poly (ethylene-co-vinyl acetate) (EVA) composites for food packaging applications: A study based on barrier and biodegradation behavior," *Journal of Food Engineering*, vol. 118, no. 1, pp. 78–89, Sep. 2013, doi: 10.1016/j.jfoodeng.2013.03.020.

[57] N. Nordin, S. H. Othman, R. K. Basha, and S. A. Rashid, "Mechanical and thermal properties of starch films reinforced with microcellulose fibres," *Food Research*, vol. 2, no. 6, pp. 555–563, Dec. 2018, doi: 10.26656/fr.2017.2(6).110.

[58] J. M. Rajwade, K. M. Paknikar, and J. V. Kumbhar, "Applications of bacterial cellulose and its composites in biomedicine," *Applied Microbiology and Biotechnology*, vol. 99, pp. 2491–2511, Mar. 2015, doi: 10.1007/s00253-015-6426-3.

[59] A. Iskalieva et al., "Biodegradable poly(vinyl alcohol)/starch films crosslinked with itaconic acid for sustainable packaging applications," *Chemistry & Biodiversity*, vol. 23, no. 3, Mar. 2026, Art. no. e03824, doi: 10.1002/cbdv.202503824.

[60] K. Moraczewski, M. Stepczyńska, A. Raszkowska-Kaczor, L. Szymańska, and P. Rytlewski, "PLA/PCL polymer material for food packaging with enhanced antibacterial properties," *Polymers*, vol. 17, no. 9, 2025, Art. no. 1134, doi: 10.3390/polym17091134.

[61] T. Chu, J. Shi, Y. Xia, H. Wang, G. Fan, and M. Yang, "Development of high strength potato starch nanocomposite films with excellent UV-blocking performance: Effect of heat moisture treatment synergistic with ligninsulfonic acid," *Industrial Crops and Products*, vol. 187, Nov. 2022, Art. no. 115327, doi: 10.1016/j.indcrop.2022.115327.

[62] S. Agarwal, "Major factors affecting the characteristics of starch based biopolymer films," *European Polymer Journal*, vol. 160, Nov. 2021, Art. no. 110788, doi: 10.1016/j.eurpolymj.2021.110788.

[63] F. H. Santos, L. E. Siqueira, G. P. Cardoso, G. Molina, and F. M. Pelissari, "Antioxidant packaging development and optimization using agroindustrial wastes," *Journal of Applied Polymer Science*, vol. 138, no. 35, Sep. 2021, Art. no. 50887, doi: 10.1002/app.50887.

[64] R. S. Ayu et al., "Effect of Empty Fruit Bunch reinforcement in PolyButylene-Succinate/Modified Tapioca Starch blend for Agricultural Mulch Films," *Scientific Reports*, vol. 10, 2020, Art. no. 1166, doi: 10.1038/s41598-020-58278-y.

[65] J. Tarique, S. M. Sapuan, and A. Khalina, "Effect of glycerol plasticizer loading on the physical, mechanical, thermal, and barrier properties of arrowroot (*Maranta arundinacea*) starch biopolymers," *Scientific Reports*, vol. 11, 2021, Art. no. 13900, doi: 10.1038/s41598-021-93094-y.

[66] F. Xie, E. Pollet, P. J. Halley, and L. Avérous, "Starch-based nano-biocomposites," *Progress in Polymer Science*, vol. 38, no. 10–11, pp. 1590–1628, 2013, doi: 10.1016/j.progpolymsci.2013.05.002.

[67] S. B. Nunes et al., "Development of bacterial cellulose biocomposites combined with starch and collagen and evaluation of their properties," *Materials*, vol. 14, no. 2, 2021, Art. no. 458, doi: 10.3390/ma14020458.

[68] M. S. Reza, M. S. I. Tutul, T. Khandaker, C. Paul, M. M.-U. Haque, and M. S. Hossain, "Eco-friendly starch-nanocellulose bio-nanocomposite films with improved structure–property interactions," *Nanoscale Advances*, vol. 8, no. 13, pp. 3794–3803, Jul. 2026, doi: 10.1039/d6na00060f.

[69] N. E.-A. El-Naggar, S. E. El-Malkey, M. A. Abu-Saied, and A. B. A. Mohammed, "Exploration of a novel and efficient source for production of bacterial nanocellulose, bioprocess optimization and characterization," *Scientific Reports*, vol. 12, 2022, Art. no. 18533, doi: 10.1038/s41598-022-22240-x.

[70] S. Galus and J. Kadzińska, "Moisture sensitivity, optical, mechanical and structural properties of whey protein-based edible films incorporated with rapeseed oil," *Food Technology and Biotechnology*, vol. 54, no. 1, pp. 78–89, 2016, doi: 10.17113/ftb.54.01.16.3889.

[71] N. A. Tassew, T. L. Andualem, R. P. D M, M. A. Endeshaw, and R. Ramesh, "Avocado seed starch bioplastic film reinforced with enset

cellulose for sustainable packaging," *Scientific Reports*, vol. 15, 2025, Art. no. 41075, doi: 10.1038/s41598-025-24935-3.

[72] M. T. Hossain, M. A. Shahid, M. G. M. Limon, I. Hossain, and N. Mahmud, "Techniques, applications, and challenges in textiles for a sustainable future," *Journal of Open Innovation: Technology, Market, and Complexity*, vol. 10, no. 1, Mar. 2024, Art. no. 100230, doi: 10.1016/j.joitmc.2024.100230.

[73] C. Rong-or, W. Pongputthipat, Y. Ruksakulpiwat, and P. Chumsamrong, "Soil burial degradation of bio-composite films from poly(lactic acid), natural rubber, and rice straw," *Polymer Bulletin*, vol. 81, pp. 10729–10746, Aug. 2024, doi: 10.1007/s00289-024-05229-6.

[74] J. Nilsen-Nygaard et al., "Current status of biobased and biodegradable food packaging materials: Impact on food quality and effect of innovative processing technologies," *Comprehensive Reviews in Food Science and Food Safety*, vol. 20, no. 2, pp. 1333–1380, Mar. 2021, doi: 10.1111/1541-4337.12715.

[75] X. Liu et al., "Effect of biaxial stretching on the microstructure evolution, optical, mechanical and oxygen barrier properties of biodegradable poly(lactic acid) (PLA)/poly(butylene adipate-co-terephthalate) (PBAT) films," *International Journal of Biological Macromolecules*, vol. 253, Dec. 2023, Art. no. 126976, doi: 10.1016/j.ijbiomac.2023.126976.

[76] M. J. Bof, D. E. Locaso, and M. A. García, "Corn starch-chitosan proportion affects biodegradable film performance for food packaging purposes," *Starch - Stärke*, vol. 73, no. 5–6, May 2021, Art. no. 2000104, doi: 10.1002/star.202000104.

[77] S. Gea, K. M. Pasaribu, A. A. Sarumaha, and S. Rahayu, "Cassava starch/bacterial cellulose-based bioplastics with Zanthoxylum acanthopodium," *Biodiversitas*, vol. 23, no. 5, pp. 2601–2608, May 2022, doi: 10.13057/biodiv/d230542.

[78] P. Cazón and M. Vázquez, "Bacterial cellulose as a biodegradable food packaging material: A review," *Food Hydrocolloids*, vol. 113, Apr. 2021, Art. no. 106530, doi: 10.1016/j.foodhyd.2020.106530.

[79] M. Vázquez, G. Velazquez, and P. Cazón, "UV-Shielding films of bacterial cellulose with glycerol and chitosan. Part 2: Structure, water vapor permeability, spectral and thermal properties," *CyTA - Journal of Food*, vol. 19, no. 1, pp. 115–126, 2021, doi: 10.1080/19476337.2020.1870565.

[80] R. Santhosh and P. Sarkar, "Jackfruit seed starch/tamarind kernel xyloglucan/zinc oxide nanoparticles-based composite films: Preparation, characterization, and application on tomato (*Solanum lycopersicum*) fruits," *Food Hydrocolloids*, vol. 133, Dec. 2022, Art. no. 107917, doi: 10.1016/j.foodhyd.2022.107917.

[81] S. S. Ali et al., "Bioplastic production in terms of life cycle assessment: A state-of-the-art review," *Environmental Science and Ecotechnology*, vol. 15, Jul. 2023, Art. no. 100254, doi: 10.1016/j.ese.2023.100254.